Physica D 240 (2011) 389–396

Contents lists available at ScienceDirect

Physica D

journal homepage: www.elsevier.com/locate/physd

Fermi acceleration and its suppression in a time-dependent Lorentz gas

Diego F.M. Oliveira [a,b,*], Jürgen Vollmer [a], Edson D. Leonel [c]

[a] Max Planck Institute for Dynamics and Self-Organization, Bunsenstrasse 10, D-37073, Göttingen, Germany

[b] CAMTP—Center for Applied Mathematics and Theoretical Physics, University of Maribor, Krekova 2, SI-2000 Maribor, Slovenia

[c] Departamento de Estatística, Matemática Aplicada e Computação, Instituto de Geociências e Ciências Exatas, Universidade Estadual Paulista, Av. 24A, 1515, Bela Vista, CEP: 13506-900, Rio Claro, SP, Brazil

ARTICLE INFO

Article history:
Received 27 March 2010
Received in revised form
29 September 2010
Accepted 30 September 2010
Available online 8 October 2010
Communicated by Y. Nishiura

Keywords:
Billiard
Lorentz gas
Lyapunov exponents
Fermi acceleration
Scaling

ABSTRACT

Some dynamical properties for a Lorentz gas were studied considering both static and time-dependent boundaries. For the static case, it was confirmed that the system has a chaotic component characterized with a positive Lyapunov exponent. For the time-dependent perturbation, the model was described using a four-dimensional nonlinear map. The behaviour of the average velocity is considered in two different situations: (i) non-dissipative and (ii) dissipative dynamics. Our results confirm that unlimited energy growth is observed for the non-dissipative case. However, and totally new for this model, when dissipation via inelastic collisions is introduced, the scenario changes and the unlimited energy growth is suppressed, thus leading to a phase transition from unlimited to limited energy growth. The behaviour of the average velocity is described using scaling arguments.

1. Introduction

The process in which a classical particle acquires unlimited energy from collisions with heavy and moving boundaries is often called the phenomenon of Fermi acceleration. It was first reported by Enrico Fermi [1] as an attempt to explain the acceleration of cosmic rays. He proposed that such behaviour appears due to interaction between charged particles and time-dependent magnetic fields produced by the interstellar medium. Later, [1] some alternative models have been proposed using different approaches with applications in different fields of science including molecular physics [2], optics [3], nanostructures [4], quantum dots [5] and many other.

One of the most studied versions of the problem is the well known one-dimensional Fermi–Ulam model (FUM) [6–12]. The model consists of a classical particle confined and bouncing between two rigid walls in which one of them is fixed and the other one moves in time according to a periodic function. It is well known that the phase space, in the absence of dissipation, shows a mixed structure in the sense that depending on the combinations of control parameters and initial conditions, both invariant spanning curves (also called invariant tori), chaotic seas and Kolmogorov–Arnold–Moser (KAM) islands are all observed. An alternative model was later proposed by Pustylnikov [13,14]. Such a system consists of a classical particle bouncing in a vertical moving platform under the effect of an external constant gravitational field [15–21]. Despite the similarity between the two models, they exhibit different behaviour for the average velocity for long time. The main difference between them is that in the FUM framework the Fermi acceleration is not observed. The time between two collisions decreases as the velocity increases. On the other hand, for specific combinations of both control parameters and initial conditions the phenomenon of unlimited energy growth can be observed in the bouncer model. For such a model, the time between collisions rises as the velocity increases, thus leading the particle to experience a loss of correlation between two collisions thus leading to Fermi acceleration. This apparently contradictory result was later discussed and explained by Lichtenberg and Lieberman [22,23] and can be easily understood by looking at the phase space. The FUM has a set of invariant spanning curves limiting the size of the chaotic sea (as well as the particle's velocity), but such invariant tori, which could be interpreted as physical barriers, are not observed in the bouncer model and the energy grows unbounded. Extensions of the formalism for two dimensional systems are not so simple, thus one cannot confirm *a priori* if the phenomenon of Fermi acceleration will be observed or not. In this sense a conjecture was proposed by Loskutov–Ryabov–Akinshin (LRA) [24]. This conjecture, known as the LRA-conjecture, states that a chaotic

* Corresponding author at: CAMTP—Center for Applied Mathematics and Theoretical Physics, University of Maribor, Krekova 2, SI-2000, Maribor, Slovenia.
E-mail addresses: diegofregolente@gmail.com (D.F.M. Oliveira), juergen.vollmer@ds.mpg.de (J. Vollmer), edleonel@rc.unesp.br (E.D. Leonel).

0167-2789/$ – see front matter © 2010 Elsevier B.V. All rights reserved.
doi:10.1016/j.physd.2010.09.015

component in the phase space with static boundary is a sufficient condition to observe Fermi acceleration when a perturbation is introduced. Results that corroborate the validity of this conjecture include the time-dependent oval billiard [25] and stadium billiard [26]. Very recent Leonel and Bunimovich [27] extended the conjecture for the existence of a heteroclinic orbit in the phase space instead of the existence of a set with chaotic dynamics.

When dissipation is introduced, a drastic change is observed in the phase space. Invariant spanning curves are destroyed; the elliptic fixed points turns into sinks and the chaotic sea can be eventually replaced by a chaotic attractor [28]. However, the influence of dissipation on the average velocity is still not fully understood. Some consequences of the dissipation to the phenomenon of Fermi acceleration in a one-dimensional Fermi–Ulam model were discussed by Leonel [29]. It is well known that in such a system, in its original formulation and for smooth enough perturbation of the boundary, the particle does not have unlimited energy growth. If one considers the motion of the moving wall to be random, the phenomenon of Fermi acceleration is observed. However, the introduction of inelastic collision is enough to suppress Fermi acceleration. Results considering also the one dimensional Fermi–Ulam model under an external force of sawtooth type [30] under effects of dissipation generated from sliding of a body against a rough surface have also been considered. The external perturbation of sawtooth type was chosen because the oscillating wall always gives energy to the particle after collisions. The main question they addressed was: *would it be possible to suppress Fermi acceleration under the effect of dissipation generated from sliding of a body against a rough surface?* The answer is not so simple and it depends on both initial conditions and the combination of control parameters. It was observed that for a certain range of parameters Fermi acceleration can be observed. But then, it is suppressed under specific ranges of initial conditions.

In this paper, we study a Lorentz gas model considering both the static and the time-dependent boundary. In the first part of the paper, we study the Lorentz gas with static boundary. We derive a two dimensional nonlinear mapping that describes the dynamics of the model. We obtain the phase space and we show that it has chaotic components which are characterized via a positive Lyapunov exponent. Then, in the second part, we introduce a time-dependent perturbation to the boundary. There are many different ways to introduce a time-dependent perturbation and the most common methods are: (i) the stochastic case, where the boundary changes according to a random function [29]; (ii) the regular case, where the position of the boundary varies according to a harmonic law [31]. However, in both situations the position of the centre of mass of the discs, which describe the scatterers, is assumed to be fixed. Then, for the first time, we introduce a different kind of time-dependent perturbation for a Lorentz gas. We assume that the radius of the scatterers is fixed and the centre of mass changes according to a harmonic function. Our main goal in this part of the work is to verify the validity of the LRA conjecture (see also Ref. [27] for a new writing of the LRA conjecture), which is confirmed when we studied the behaviour of the average velocity for an ensemble of particles. Since the phenomenon of Fermi acceleration is present in this model our next approach is to introduce dissipation into the model via damping coefficients and try to understand the influence of dissipation on the particle's behaviour. Our results allow us to confirm that when inelastic collisions are introduced into the model, such a procedure is a sufficient condition to break down the phenomenon of Fermi acceleration [29]. In both the conservative as well as the dissipative cases, we describe the behaviour of the average velocity using a scaling formalism.

The paper is organized as follows. In Section 2 we describe how to obtain the two-dimensional mapping that describes the dynamics of the static system. Section 3 is devoted to discussing the time-dependent model as well as our numerical results. Finally the conclusions are drawn in Section 4.

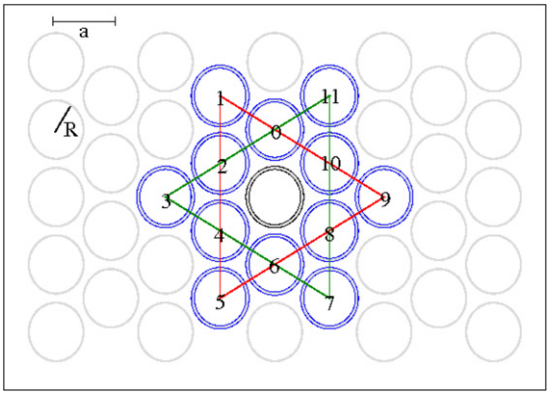

Fig. 1. Illustration of the Lorentz gas with triangular configuration.

2. A static Lorentz gas and the mapping

In this section we discuss all the details needed for the construction of a nonlinear mapping that describes the dynamics of the problem. The model consists of a classical particle of mass m suffering elastic collisions with circular scatterers (see Fig. 1). We chose a triangular arrangement of the scatterers [32] (which also appears as the Star of David if one connects circles 1, 5 and 9 and 11, 7 and 3) in order to avoid particles travelling infinitely far between collisions, and the fixed lattice spacing a to be twice the radius of the scatterers, $R = a/2$. The system is described in terms of a two dimensional mapping $\Xi(\theta_n, b_n) = (\theta_{n+1}, b_{n+1})$ where the dynamical variable θ_n denotes the direction of the trajectory while b_n is the impact parameter. Given an initial condition (θ_0, b_0), the particle starts from the black circle (centre in Fig. 1) and hits one of the 12 other circles. In this sense, we specify the scattered hit in the collision $n+1$ by $s_n = 0, \ldots, 11$ and introduce $l(s_n)$ for the distance between this scatterer and the scatterer hit at the collision $n+1$. $l(s_n)$ can assume the values of $2a/\sqrt{3}$ and $2a$ for even and odd values of s_n, respectively. Additionally, when the particle hits the boundary it is specularly reflected with the same absolute velocity. The particle does not suffer influences of any external field along its linear trajectory. From the green triangle in Fig. 2(a) one can easily verify

$$\sin\left(\theta_n - \frac{\pi s_n}{6}\right) = -\frac{(b_{n+1} - b_n)}{l(s_n)}. \tag{1}$$

Moreover, from Fig. 2(b) one can find that

$$\alpha = \arcsin(-b_{n+1}/R), \tag{2}$$
$$\beta = \pi - 2\alpha, \tag{3}$$
$$\psi = 2\alpha - \theta_n, \tag{4}$$
$$\theta_{n+1} = \pi - 2\alpha + \theta_n. \tag{5}$$

Such a result allows us to obtain θ_{n+1},

$$\theta_{n+1} = \pi + \theta_n + 2\arcsin(b_{n+1}/R). \tag{6}$$

From Eq. (1) it is easily to find that the impact parameter, b_{n+1}, is given by

$$b_{n+1} = b_n - l(s_n)\sin\left(\theta_n - \frac{\pi s_n}{6}\right). \tag{7}$$

Thus, the mapping that describes the dynamics of a two dimensional Lorentz gas is given by

$$\Xi : \begin{cases} \theta_{n+1} = \pi + \theta_n + 2\arcsin\left(\dfrac{b_{n+1}}{R}\right) \\ b_{n+1} = b_n - l(s_n)\sin\left(\theta_n - \dfrac{\pi s_n}{6}\right) \end{cases}, \tag{8}$$

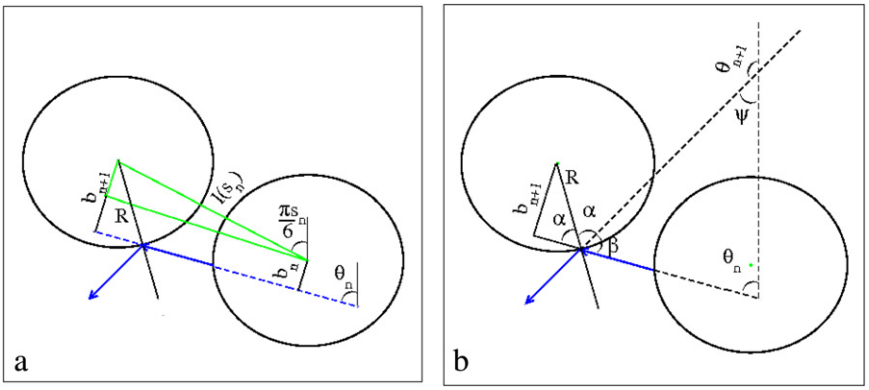

Fig. 2. Dependence of (a) b_{n+1} on b_n and θ_n; (b) θ_{n+1} on b_{n+1} and θ_n.

by definition $b \in [-R, R]$ and $\theta \in [0, 2\pi]$ is a counterclockwise angle such that Ξ is defined on the fundamental domain $[-R, R] \times [0, 2\pi]$. From the mapping Ξ, Eq. (8), one can easily obtain the Jacobian matrix, J, which is defined as

$$J = \begin{pmatrix} \frac{\partial\theta_{n+1}}{\partial\theta_n} & \frac{\partial\theta_{n+1}}{\partial b_n} \\ \frac{\partial b_{n+1}}{\partial\theta_n} & \frac{\partial b_{n+1}}{\partial b_n} \end{pmatrix}, \tag{9}$$

with coefficients given by

$$\frac{\partial\theta_{n+1}}{\partial\theta_n} = 1 - 2\sqrt{R^2 - b_{n+1}^2}\, l(s_n) \cos\left(\theta_n - \frac{\pi s_n}{6}\right), \tag{10}$$

$$\frac{\partial\theta_{n+1}}{\partial b_n} = 2\sqrt{R^2 - b_{n+1}^2}, \tag{11}$$

$$\frac{\partial b_{n+1}}{\partial\theta_n} = -l(s_n) \cos\left(\theta_n - \frac{\pi s_n}{6}\right), \tag{12}$$

$$\frac{\partial b_{n+1}}{\partial b_n} = 1. \tag{13}$$

After some easy calculation one can show that the mapping Ξ preserves the phase space measure since $\det(J) = 1$.

It is well known that the Lyapunov exponents are an important tool to identify whether the model has chaotic regions or not. As discussed in [33], the Lyapunov exponents are defined as

$$\lambda_j = \lim_{n\to\infty} \frac{1}{n} \ln |\Lambda_j|, \quad j = 1, 2, \tag{14}$$

where Λ_j are the eigenvalues of $M = \prod_{i=1}^{n} J_i(\theta_i, b_i)$ and J_i is the Jacobian matrix evaluated over the orbit (θ_i, b_i). However, direct implementation of a computational algorithm to evaluate Eq. (14) has severe limitations in obtaining M. Even in the limit of short n, the components of M can assume very different orders of magnitude for chaotic orbits and periodic attractors making impractical the implementation of the algorithm. In order to avoid this problem we note that J can be written as $J = \Theta T$ where Θ is an orthogonal matrix and T is a right triangular matrix. Thus we rewrite M as $M = J_n J_{n-1} \ldots J_2 \Theta_1 \Theta_1^{-1} J_1$, where $T_1 = \Theta_1^{-1} J_1$. A product of $J_2\Theta_1$ defines a new J_2'. In a next step, it is easy to show that $M = J_n J_{n-1} \ldots J_3 \Theta_2 \Theta_2^{-1} J_2' T_1$. The same procedure can be used to obtain $T_2 = \Theta_2^{-1} J_2'$ and so on. Using this procedure the problem is reduced to evaluate the diagonal elements of $T_i : T_{11}^i$, T_{22}^i. Finally, the Lyapunov exponents are now given by

$$\lambda_j = \lim_{n\to\infty} \frac{1}{n} \sum_{i=1}^{n} \ln |T_{jj}^i|, \quad j = 1, 2. \tag{15}$$

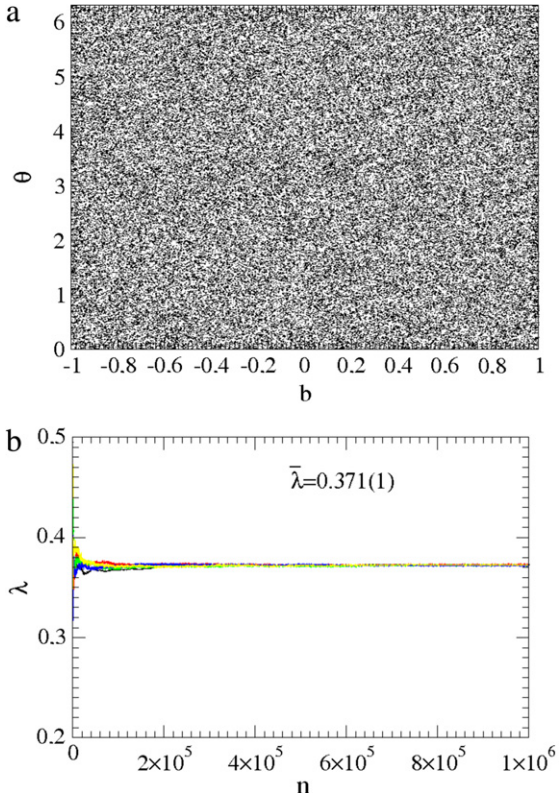

Fig. 3. (a) Phase space generated from iteration of mapping (8); (b) behaviour of the positive Lyapunov exponent of the chaotic sea. The control parameter used in both figures was $a = 2$.

If at least one of the λ_j is positive then the orbit is classified as chaotic. Additionally, in conservative systems $\lambda_1 + \lambda_2 = 0$ while in dissipative systems $\lambda_1 + \lambda_2 < 0$, which is a consequence of the Liouville's theorem. The phase space for the mapping (8) is shown in Fig. 3(a). For the same control parameter used in Fig. 3(a), $a = 2$, we have also evaluated numerically the positive Lyapunov exponent as one can see in Fig. 3(b). The average of the positive Lyapunov exponent for the ensemble of the five time series gives $\bar{\lambda} = 0.371 \pm 0.001$ where the value 0.001 corresponds to the standard deviation of the five samples.

So as a main conclusion of this section, we confirm that the static version of the Lorentz gas does indeed have chaotic portions therefore leading one to believe, according to the LRA conjecture, that if a time-dependent perturbation to the boundary is introduced, then Fermi acceleration should be observed.

3. A time-dependent Lorentz gas

In this section we introduce for the first time in the literature, a new kind of time-dependent perturbation in a Lorentz gas. We assume that the radius of the scatterers is fixed and the centre of mass changes according to a harmonic function $f(t)$, in particular we assume the case where

$$f_i(t) = \epsilon_i[1 + \cos(t)], \quad \text{for } i = x, y \tag{16}$$

where ϵ_i is the amplitude of the time-dependent perturbation and t is the time. As a consequence of the introduction of the time-dependent perturbation into the model, two new dynamical variables appear namely, velocity and time. Such a new set of variables leads us to describe the system in terms of a four dimensional nonlinear mapping which relates the nth collision to the $(n+1)$th as $\Xi(\theta_n, b_n, V_n, t_n) = (\theta_{n+1}, b_{n+1}, V_{n+1}, t_{n+1})$. The corresponding variables are: (i) the direction of the trajectory, θ_n; (ii) the impact parameter, b_n; (iii) the absolute velocity of the particle, V_n and (iv) the instant of the collision with the boundary, t_n.

Assuming that an initial condition $(\theta_0, b_0, V_0, t_0)$ is given, we can obtain the equation that describes the dynamics of the system. Thus, according to our construction, the Cartesian components of R are given by

$$X(\delta_n, t_n) = R\cos(\delta_n) + \epsilon_x[1 + \cos(t_n)], \tag{17}$$

$$Y(\delta_n, t_n) = R\sin(\delta_n) + \epsilon_y[1 + \cos(t_n)], \tag{18}$$

where δ_n is the angular position which is given by $\delta_n = \pi/2 + \theta_n - \arcsin(b_n/R)$. Since we already know the angle that the particle's trajectory makes with the horizontal $(\theta_n + \pi/2)$ and the position of the hit at the nth collision, a velocity vector can be obtained and is written as

$$\overrightarrow{V}_n = |\overrightarrow{V_n}|[\cos(\theta_n + \pi/2)\widehat{i} + \sin(\theta_n + \pi/2)\widehat{j}], \tag{19}$$

where $\widehat{i}$ and $\widehat{j}$ represent the unit vectors with respect to the X and Y coordinates, respectively. The above expressions allow us to obtain the position of the particle as a function of time for $t \geq t_n$, thus

$$X_p(t) = X(\delta_n, t_n) + |\overrightarrow{V}_n|\cos(\theta_n + \pi/2)(t - t_n), \tag{20}$$

$$Y_p(t) = Y(\delta_n, t_n) + |\overrightarrow{V}_n|\sin(\theta_n + \pi/2)(t - t_n). \tag{21}$$

The index p denotes the corresponding coordinates of the particle. In order to know the position of the particle at the $(n+1)$th collision we need to solve numerically the following equation

$$r = \sqrt{[X_x(t) - X_p(t)]^2 + [Y_y(t) - Y_p(t)]^2} \cong R, \tag{22}$$

where both X_x and Y_y are given by

$$X_x(t) = l_x + \epsilon_x[1 + \cos(t)], \tag{23}$$

$$Y_y(t) = l_y + \epsilon_y[1 + \cos(t)], \tag{24}$$

with l_x and l_y the X and Y components of $l(s_n)$; this distance is measured from the origin of the coordinate system to the centre of the $s_n = 0, \ldots, 11$ scatters at the $(n+1)$th collision. Since we already know the position of the particle at the $(n+1)$th collision, then the distance between two successive impacts can be easily obtained, which is given by $d = \sqrt{[X_p(t) - X(\delta_n, t_n)]^2 + [Y_p(t) - Y(\delta_n, t_n)]^2}$. The time at the $(n+1)$th collision is obtained evaluating the expression

$$t_{n+1} = t_n + \frac{\sqrt{[X_p(t) - X(\delta_n, t_n)]^2 + [Y_p(t) - Y(\delta_n, t_n)]^2}}{|\overrightarrow{V}_n|}. \tag{25}$$

The next step is to obtain the impact parameter, b_{n+1}, which is given by

$$b_{n+1} = b_n - l(s_n)\sin\left(\theta_n - \psi + \frac{\pi}{2}\right), \tag{26}$$

where $l(s_n) = \sqrt{(\Delta X)^2 + (\Delta Y)^2}$ and $\psi = \arctan(\Delta X/\Delta Y)$ with

$$\Delta X = l_x + \epsilon_x[\cos(t_{n+1}) - \cos(t_n)] \tag{27}$$

$$\Delta Y = l_y + \epsilon_y[\cos(t_{n+1}) - \cos(t_n)] \tag{28}$$

Moreover, the new direction of the trajectory, θ_{n+1} is

$$\theta_{n+1} = \pi + \theta_n + 2\arcsin\left[\frac{b_{n+1}}{R}\right]. \tag{29}$$

We already know $(\theta_{n+1}, b_{n+1}, t_{n+1})$; however, we still have to find $\overrightarrow{V}_{n+1}$. At the new angular position δ_{n+1}, the unitary tangent and normal vectors are

$$\overrightarrow{T}_{n+1} = \cos(\delta_{n+1})\widehat{i} + \sin(\delta_{n+1})\widehat{j}, \tag{30}$$

$$\overrightarrow{N}_{n+1} = -\sin(\delta_{n+1})\widehat{i} + \cos(\delta_{n+1})\widehat{j}. \tag{31}$$

Since the reference frame of the boundary is moving, then, at the instant of the collision, according to our construction, the following conditions must be satisfied

$$\overrightarrow{V'}_{n+1} \cdot \overrightarrow{T}_{n+1} = \gamma\,\overrightarrow{V'}_n \cdot \overrightarrow{T}_{n+1}, \tag{32}$$

$$\overrightarrow{V'}_{n+1} \cdot \overrightarrow{N}_{n+1} = -\delta\,\overrightarrow{V'}_n \cdot \overrightarrow{N}_{n+1}, \tag{33}$$

where $\gamma \in [0, 1]$ and $\delta \in [0, 1]$ are damping coefficients, which means that the particle has a fractional loss of energy upon each collision. The complete inelastic case occurs when $\gamma = \delta = 0$. On the other hand, when $\gamma = \delta = 1$ corresponds to the conservative case. The upper prime indicates that the velocity of the particle is measured with respect to the moving boundary referential frame.

Hence, one can easily find that

$$\overrightarrow{V}_{n+1} \cdot \overrightarrow{T}_{n+1} = \gamma\,\overrightarrow{V}_n \cdot \overrightarrow{T}_{n+1} + (1 - \gamma)\,\overrightarrow{V}_b(t_{n+1}) \cdot \overrightarrow{T}_{n+1}, \tag{34}$$

$$\overrightarrow{V}_{n+1} \cdot \overrightarrow{N}_{n+1} = -\delta\,\overrightarrow{V}_n \cdot \overrightarrow{N}_{n+1} + (1 + \delta)\,\overrightarrow{V}_b(t_{n+1}) \cdot \overrightarrow{N}_{n+1}, \tag{35}$$

where $\overrightarrow{V}_b(t_{n+1})$ is the velocity of the boundary which is written as

$$\overrightarrow{V}_b(t_{n+1}) = -\sin(t_{n+1})[\epsilon_x\widehat{i} + \epsilon_y\widehat{j}]. \tag{36}$$

Finally, the velocity at the $(n+1)$th collision is given by

$$|\overrightarrow{V}_{n+1}| = \sqrt{(\overrightarrow{V}_{n+1} \cdot \overrightarrow{T}_{n+1})^2 + (\overrightarrow{V}_{n+1} \cdot \overrightarrow{N}_{n+1})^2}. \tag{37}$$

3.1. Numerical results

As part of our numerical results for the time-dependent Lorentz gas, we shall discuss the behaviour of the average velocity of the particle, thus the phenomenon of Fermi acceleration. Two different procedures were applied in order to obtain the average velocity. First, we evaluate the average velocity over the orbit for a single initial condition which is defined as

$$V_i = \frac{1}{n+1}\sum_{j=0}^{n} V_{i,j}, \tag{38}$$

where the index i corresponds to a sample of an ensemble of initial conditions. Hence, the average velocity is written as

$$\overline{V} = \frac{1}{M}\sum_{i=1}^{M} V_i, \tag{39}$$

where M denotes the number of different initial conditions. We have considered $M = 1000$ in our simulations and from now on, we also fixed the value $a = 2$.

3.2. Scaling results for the conservative case

It is natural to believe that as the control parameters are varied, the behaviour of the average velocity may depend explicitly on

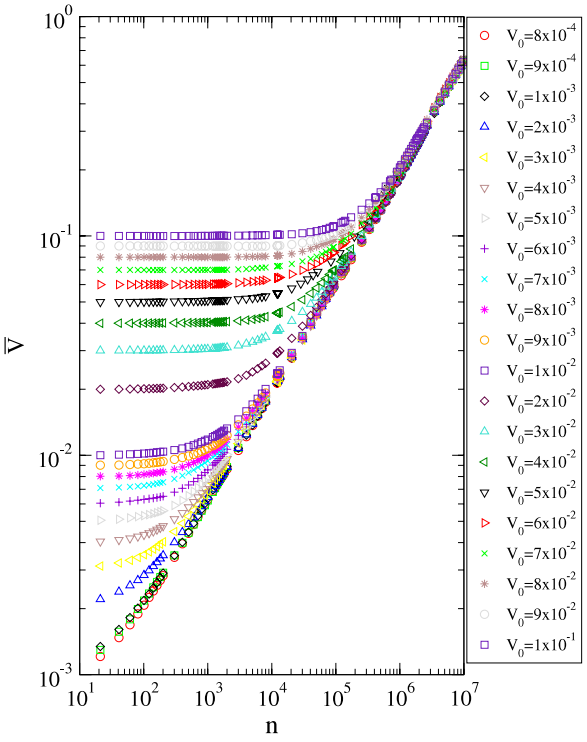

Fig. 4. Behaviour of $\bar{V} \times n$ for different initial velocities. The control parameters used were $\epsilon_x = 10^{-4}$, $\epsilon_y = 3 \times 10^{-4}$ and $a = 2$.

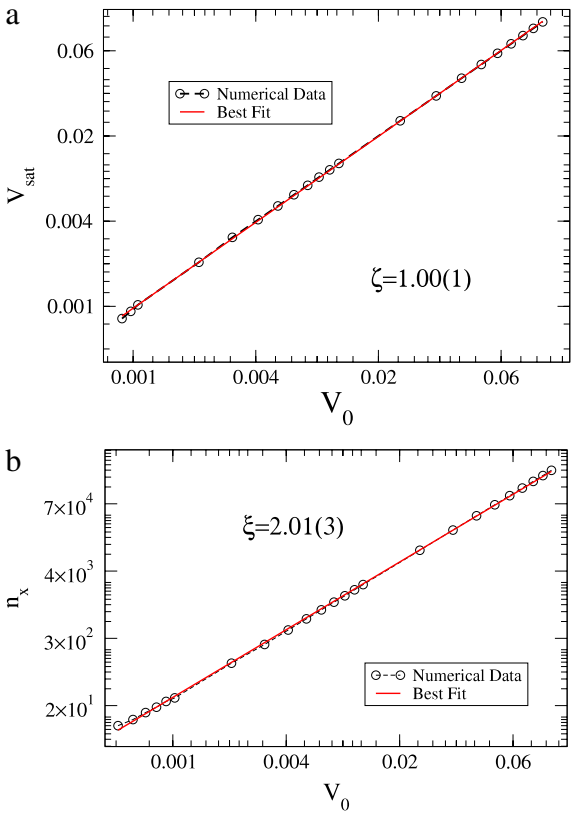

Fig. 5. (a) Plot of $V_{sat} \times V_0$. (b) Behaviour of n_x as a function of V_0.

them [34–36]. In this section we discuss the influence of the initial velocity on the behaviour of the average velocity, thus our main goal in this section is to describe a scaling present in the model for the conservative case. We assume in Eqs. (32) and (33) that $\gamma = \delta = 1$. Such a set of control parameters lets us confirm the applicability of the LRA conjecture to this model (see Ref. [27] for a new version of the LRA conjecture).

We begin by discussing a scaling observed for the average velocity of the particle as a function of V_0 and n. Fig. 4 shows the behaviour of $\bar{V} \times n$ for different initial velocities. The control parameters used in Fig. 4 were $\epsilon_x = 10^{-4}$ and $\epsilon_y = 3 \times 10^{-4}$. We have chosen 21 different values for V_0 while a random choice for the other variables were made as $t \in [0, 2\pi]$, $\theta \in [0, 2\pi]$ and $b \in [1 - (\epsilon_x + \epsilon_y), -1 + (\epsilon_x + \epsilon_y)]$. As one can see, all curves of $\bar{V}$ behave quite similarly in the sense that: (a) for short n, the average velocity remains constant for a while when eventually, (b) after a changeover, all the curves start growing with the same exponent. Such behaviour is typical in systems that can be described using the scaling approach. Based on the behaviour shown in Fig. 4, we propose the following hypotheses:

1. when $n \ll n_x$, $\bar{V}$ behaves according to

$$\bar{V}_{sat} \propto V_0^{\zeta}, \tag{40}$$

2. for $n \gg n_x$, the average velocity is given by

$$\bar{V} \propto n^{\nu}, \tag{41}$$

3. the crossover iteration number that marks the change from constant velocity to the growth regime is written as

$$n_x \propto V_0^{\xi}, \tag{42}$$

where ζ and ν are the critical exponents and ξ is a dynamic exponent.

After considering these three initial suppositions, we suppose that the average velocity is described in terms of a homogeneous function of the type

$$\bar{V}(V_0, n) = \mathrm{l}\bar{V}(\mathrm{l}^p V_0, \mathrm{l}^q n), \tag{43}$$

where l is the scaling factor, p and q are scaling exponents that in principle must be related to ζ, ν and ξ. If we chose $\mathrm{l}^p V_0 = 1$, then $\mathrm{l} = V_0^{-1/p}$ and Eq. (43) is given by

$$\bar{V}(V_0, n) = V_0^{-1/p} \bar{V}_1(V_0^{-q/p} n), \tag{44}$$

where $\bar{V}_1(V_0^{-q/p} n) = \bar{V}(1, V_0^{-q/p} n)$ is assumed to be constant for $n \ll n_x$. Comparing Eqs. (44) and (40), we obtain $\zeta = -1/p$.

On the other hand, choosing now $\mathrm{l} = n^{-1/q}$, Eq. (43) is rewritten as

$$\bar{V}(V_0, n) = n^{-1/q} \bar{V}_2(n^{-p/q} V_0), \tag{45}$$

where the function $\bar{V}_2$ is defined as $\bar{V}_2(n^{-p/q} V_0) = \bar{V}(n^{-p/q} V_0, 1)$. It is also assumed to be constant for $n \gg n_x$. Comparing Eqs. (45) and (41) we find $\nu = -1/q$. Given the two different expressions of the scaling factor l, we obtain a relation for the dynamic exponent ξ, which is given by

$$\xi = \frac{\zeta}{\nu}. \tag{46}$$

Note that the scaling exponents are determined if the critical exponents ζ and ν are numerically obtained. The exponent ν is obtained from a power law fitting for the average velocity when $n \gg n_x$. Thus, an average of these values gives $\nu = 0.49(1)$. Fig. 5 shows the behaviour of (a), $\bar{V}_{sat} \times V_0$ and (b), $n_x \times V_0$. Applying power law fittings we obtain $\zeta = 1.00(1) \cong 1$ and $\xi = 2.01(3)$. Considering the previous values of both ζ and ν and using $\xi = \zeta/\nu$, we find that $\xi = 2.04(2)$. Such a result indeed agrees with our numerical data.

In order to confirm the initial hypotheses and, since the values of the scaling exponents ζ, ν and ξ are now known, we may

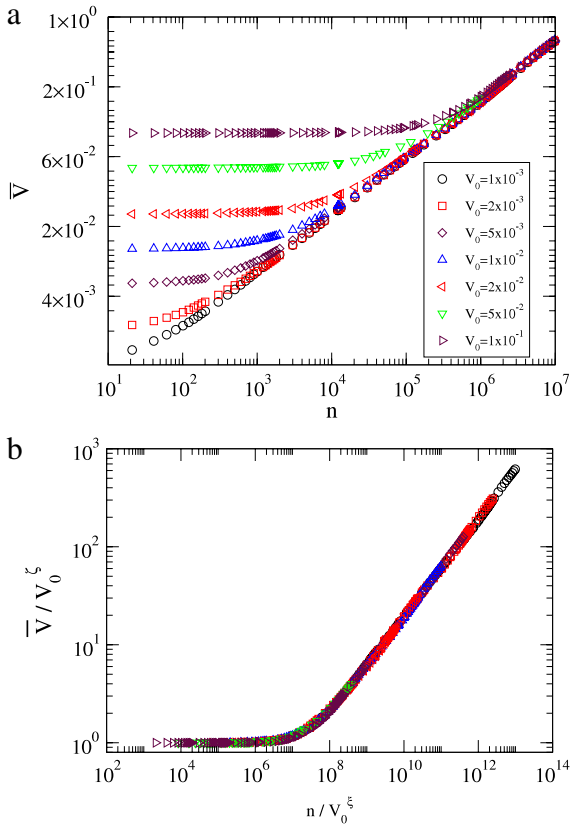

Fig. 6. (a) Behaviour of average velocity for different values of V_0; (b) their collapse onto a single and universal plot.

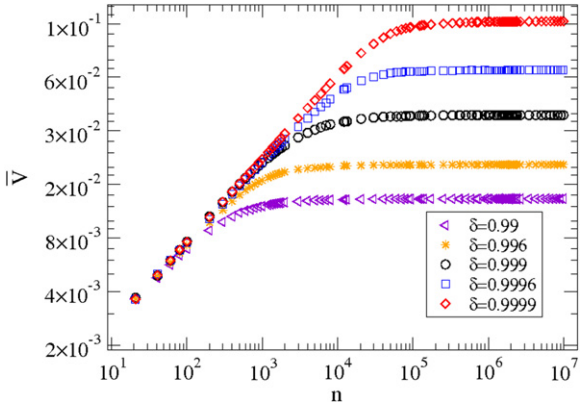

Fig. 7. Behaviour of $\overline{V} \times n$ for different values of δ, as labelled in the figure.

in principle collapse all the curves onto a single and universal plot, as demonstrated in Fig. 6. Such a collapse confirms that, despite the strong influence of the initial velocity, the behaviour of the average velocity is therefore scaling invariant under specific transformations. For large enough time, our results thus confirm that the LRA conjecture was also applied successfully in this model.

3.3. Scaling results for the dissipative case

In this section we will use the same scaling formalism as used in the previous section but now to describe the behaviour of the average velocity of the particle in the presence of dissipation. Our approach will then be to characterize the behaviour of the average velocity in terms of the number of collisions with the scatters and as a function of the damping coefficient along the normal component of the particle's velocity, δ. We study a dissipative version of the Lorentz gas close to the transition from unlimited to limited energy growth. Indeed, such a transition happens when the control parameter $\delta \to 1$ and it is better characterized if we chose the following convenient transformation $\delta \to (1-\delta)$.

To obtain the average velocity, each initial condition has a fixed initial velocity, $V_0 = 10^{-4}$ and randomly chosen $t \in [0, 2\pi]$, $\theta \in [0, 2\pi]$ and $b \in [1-(\epsilon_x+\epsilon_y), -1+(\epsilon_x+\epsilon_y)]$. The control parameter γ was fixed as $\gamma = 1$.

Fig. 7 shows the behaviour of the average velocity as a function of the number of collisions for different values of the damping coefficient δ. Observe that, for different values of δ and for small n, the average velocity starts to grow and then it bends towards a regime of saturation for large enough values of n. The changeover from growth to the saturation is marked by a typical crossover number n_x. For such a behaviour, we can also propose the following scaling hypotheses:

1. when $n \ll n_x$ the average velocity is
$$\overline{V} \propto n^{\eta}, \tag{47}$$
2. for long time, $n \gg n_x$, the average velocity approaches a regime of saturation, that is described as
$$\overline{V}_{\text{sat}} \propto (1-\delta)^{\sigma}, \tag{48}$$
3. the crossover number that marks the regime of growth to the constant velocity is written as
$$n_x \propto (1-\delta)^{z}, \tag{49}$$
where σ, η and z are critical exponents.

These scaling hypotheses allow us to describe the average velocity in terms of a scaling function of the type

$$\overline{V}[n, (1-\delta)] = l\overline{V}[l^p n, l^q(1-\delta)], \tag{50}$$

where p and q are scaling exponents and l is a scaling factor. Since l is a scaling factor, we can chose it such that $l^p n = 1$, yielding

$$\overline{V}[n, (1-\delta)] = n^{-1/p}\overline{V}_1[(n)^{-q/p}(1-\delta)], \tag{51}$$

where $\overline{V}_1[(n)^{-q/p}(1-\delta)] = \overline{V}[1, (n)^{-q/p}(1-\delta)]$ is assumed to be constant for $n \ll n_x$. Comparing Eqs. (47) and (51), we obtain $\eta = -1/p$. A power law fitting gives us that $\eta = 0.471(2)$. Such a value was obtained from the range of $\delta \in [0.99, 0.99999]$. Choosing now $l^q(1-\delta) = 1$, we have that $l = (1-\delta)^{-1/q}$ and Eq. (50) is rewritten as

$$\overline{V}[n, (1-\delta)] = (1-\delta)^{-1/q}\overline{V}_2[(1-\delta)^{-p/q}n], \tag{52}$$

where $\overline{V}_2[(1-\delta)^{-p/q}n] = \overline{V}[(1-\delta)^{-p/q}n, 1]$ is assumed to be constant for $n \gg n_x$. Comparing Eqs. (48) and (52), we obtain $-1/q = \sigma = -0.47(3)$ (see Fig. 8(a)). Using now the expressions obtained for the scaling factor l, we can easily show that

$$z = \frac{\sigma}{\eta} = 0.99(5), \tag{53}$$

which is quite close to the value obtained numerically, as shown in Fig. 8(b). A confirmation of the initial hypotheses is made by collapsing all the curves of $\overline{V} \times n$ onto a single and universal plot, as shown in Fig. 9, showing that the system is scale invariant under a specific transformation. We also have shown that dissipation causes a drastic change in the behaviour of $\overline{V}$. Note that $\delta \to 1$ implies that Eqs. (48) and (49) both diverge, thus recovering the results for the conservative case, i.e., exhibiting Fermi acceleration. However, when δ is slightly less than 1, the average velocity grows and then reaches a regime of saturation for long enough time. Our results reinforce that dissipation introduced via damping coefficients is a sufficient condition to suppress the phenomenon of Fermi acceleration, as Leonel's conjecture claims [29].

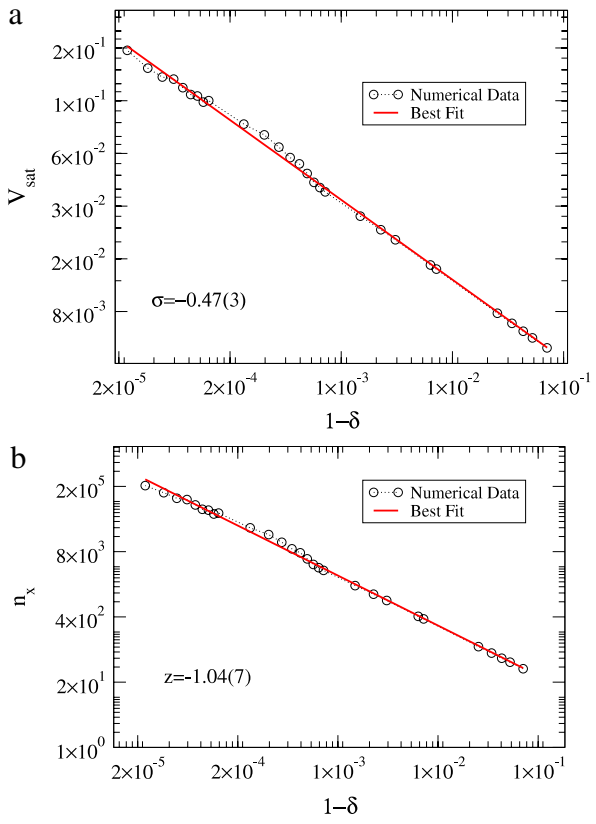

Fig. 8. (a) Behaviour of $\overline{V}_{\text{sat}} \times (1-\delta)$. (b) Behaviour of the crossover number n_x against $(1-\delta)$. A power law fitting in (a) furnishes $\sigma = -0.47(3)$ while in (b) $z = -1.04(7)$.

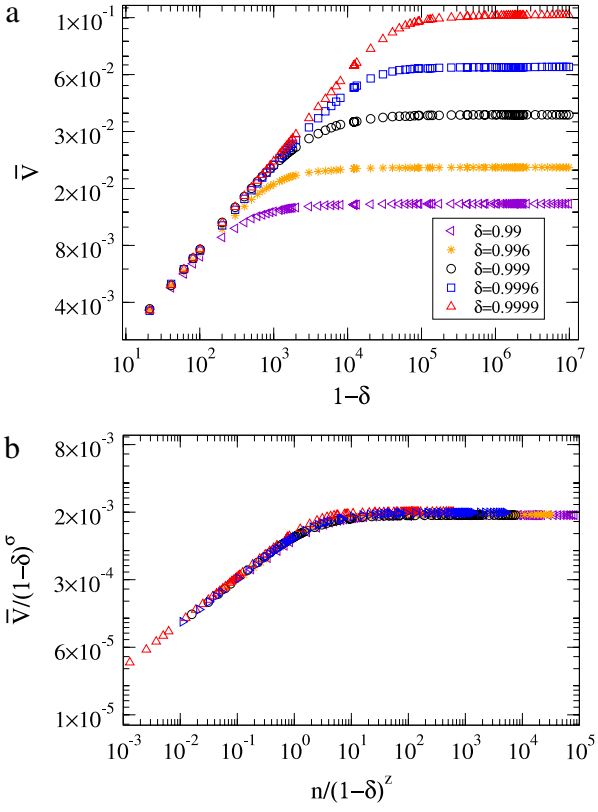

Fig. 9. (a) Different curves of $\overline{V}$ for five different control parameters. (b) Their collapse onto a single and universal plot.

4. Conclusion

In this paper we considered the problem of a classical Lorentz gas considering both static and time-dependent boundaries. For the static case we obtained the mapping that describes the dynamics of the system and we have shown that the model has a chaotic component characterized by a positive Lyapunov exponent. Such a chaotic component is what the LRA conjecture claims is needed to produce Fermi acceleration when a time-dependent perturbation to the boundary is introduced. After that, we introduce a new type of time-dependent perturbation on the boundary. Our results confirm that the LRA conjecture is applied also for the conservative case. When dissipation, via inelastic collision of the particle with the scatterers is introduced into the model, we observed that the average velocity grows with time and then reaches a constant value for large enough time confirming that Fermi acceleration is suppressed. Finally, and for the first time with this model, the average quantities were described by scaling functions with characteristic exponents whose validity was confirmed with the collapse of the curves of $\bar{V}$ into a universal plot.

Acknowledgements

D.F.M.O. gratefully acknowledges the Max Planck Institute for financial support. E.D.L. is grateful to FAPESP, CNPq and FUNDUNESP, Brazilian agencies. The authors acknowledge Dr. Douglas Fregolente and Prof. Carl P. Dettmann for a careful reading of the manuscript.

References

[1] E. Fermi, On the origin of the cosmic radiation, Phys. Rev. 75 (1949) 1169.
[2] S.E. Sklarz, D.J. Tannor, N. Khaneja, Decoherence control by tracking a Hamiltonian reference molecule, Phys. Rev. A 69 (2004) 053408.
[3] R. Gommers, S. Bergamini, F. Renzoni, Dissipation-induced symmetry breaking in a driven optical lattice, Phys. Rev. Lett. 95 (2005) 073003.
[4] M. Steiner, M. Freitag, V. Perebeinos, J.C. Tsang, J.P. Small, M. Kinoshita, D. Yuan, J. Liu, P. Avouris, Phonon populations and electrical power dissipation in carbon nanotube transistors, Nat. Nanotechnol. 4 (2009) 320.
[5] K. Nakamura, T. Harayama, Quantum Chaos and Quantum Dots, Oxford University Press, Oxford, 2004.
[6] D.G. Ladeira, J.K.L. da Silva, Time-dependent properties of a simplified Fermi–Ulam accelerator model, Phys. Rev. E 73 (2006) 026201.
[7] E.D. Leonel, J.K.L. da Silva, S.O. Kamphorst, On the dynamical properties of a Fermi accelerator model, Physica A 331 (2004) 435.
[8] A.K. Karlis, P.K. Papachristou, F.K. Diakonos, V. Constantoudis, P. Schmelcher, Hyperacceleration in a stochastic Fermi–Ulam model, Phys. Rev. Lett. 97 (2006) 194102.
[9] A.K. Karlis, P.K. Papachristou, F.K. Diakonos, V. Constantoudis, P. Schmelcher, Fermi acceleration in the randomized driven Lorentz gas and the Fermi–Ulam model, Phys. Rev. E 76 (2007) 016214.
[10] J.V. José, R. Cordery, Study of a quantum Fermi-acceleration model, Phys. Rev. Lett. 56 (1986) 290.
[11] E.D. Leonel, D.F.M. Oliveira, R.E. Carvalho, Scaling properties of the regular dynamics for a dissipative bouncing ball model, Physica A 386 (2007) 73.
[12] D.F.M. Oliveira, E.D Leonel, The Feigenbaum's δ for a high dissipative bouncing ball model, Braz. J. Phys. 38 (2008) 62.
[13] A.D. Pustylnikov, Construction of periodic-solutions in an infinite system of Fermi-pasta-Ulam ordinary diferential-equations, stability, and KAM theory, Theoret. and Math. Phys. 50 (1995) 449.
[14] A.D. Pustylnikov, On Ulam problem, Theoret. and Math. Phys. 57 (1983) 1035.
[15] P.J. Holmes, The dynamics of repeated impacts with a sinusoidally vibrating table, J. Sound Vib. 84 (1982) 173.
[16] R.M. Everson, Chaotic dynamics of a bouncing ball, Physica D 19 (1986) 355.
[17] G.A. Luna-Acosta, Regular and chaotic dynamics of the damped Fermi accelerator, Phys. Rev. A 42 (1990) 7155.
[18] E.D. Leonel, A.L.P. Livorati, Describing Fermi acceleration with a scaling approach: bouncer model revisited, Physica A 387 (2008) 1155.
[19] T.L. Vincent, A.I. Mees, Controlling a bouncing ball, J. Bifur. Chaos 10 (2000) 579.
[20] A.C.J. Luo, An unsymmetrical motion in a horizontal impact oscillator, ASME J. Vib. Acoust. 124 (2002) 420.
[21] A.C.J. Luo, R.P.S. Han, The dynamics of a bouncing ball with a sinusoidally vibrating table revisted, Nonlinear Dynam. 10 (1996) 1.
[22] A.J. Lichtenberg, M.A. Lieberman, R.H. Cohen, Fermi acceleration revisited, Physica D 1 (1980) 291.

[23] A.J. Lichtenberg, M.A. Lieberman, Regular and Chaotic Dynamics, in: Appl. Math. Sci., vol. 38, Springer Verlag, New York, 1992.
[24] A. Loskutov, A.R. Ryabov, L.G. Akinshin, Properties of some chaotic billiards with time-dependent boundaries, J. Phys. A: Math. Gen. 33 (2000) 7973.
[25] E.D. Leonel, D.F.M. Oliveira, A. Loskutov, Fermi acceleration and scaling properties of a time dependent oval billiard, Chaos 19 (2009) 033142.
[26] A.B. Ryabov, A. Loskutov, Time-dependent focusing billiards and macroscopic realization of Maxwell's Demon, J. Phys. A 43 (2010) 125104.
[27] E.D. Leonel, L.A Bunimovich, Suppressing Fermi acceleration in a driven elliptical billiard, Phys. Rev. Lett. 104 (2010) 224101.
[28] D.F.M. Oliveira, E.D. Leonel, Boundary crisis and suppression of Fermi acceleration in a dissipative two dimensional non-integrable time-dependent billiard, Phys. Lett. A 374 (2010) 3016.
[29] E.D. Leonel, Breaking down the Fermi acceleration with inelastic collisions, J. Phys. A: Math. Gen. 40 (2007) F1077.
[30] D.G. Ladeira, E.D. Leonel, Competition between suppression and production of Fermi acceleration, Phys. Rev. E (3) 81 (2010) 036216.
[31] D.G. Ladeira, J.K.L. da Silva, Scaling features of a breathing circular billiard, J. Phys. A 41 (2008) 365101.
[32] J. Vollmer, Chaos, spatial extension, transport and non-equilibrium thermodynamics, Phys. Rep. 372 (2002) 131.
[33] J.P. Eckmann, D. Ruelle, Ergodic theory of chaos and strange attractors, Rev. Modern Phys. 57 (1985) 617.
[34] D.F.M. Oliveira, E.D. Leonel, Suppressing Fermi acceleration in a two-dimensional non-integrable time-dependent oval-shaped billiard with inelastic collisions, Physica A 389 (2010) 1009.
[35] E.D. Leonel, P.V.E. McClintock, J.K.L. da Silva, Fermi–Ulam accelerator model under scaling analysis, Phys. Rev. Lett. 93 (2004) 014101.
[36] F. Lenz, F.K. Diakonos, P. Schmelcher, Phys. Rev. Lett. 100 (2008) 014103.